

## Exact solution to line source scattering by an ideal left-handed wedge

Cesar Monzon,<sup>1</sup> Donald W. Forester,<sup>2</sup> and Peter Loschialpo<sup>2</sup>

<sup>1</sup>*SFA Department NRL, Largo, Maryland 20774, USA*

<sup>2</sup>*Naval Research Laboratory, Washington, DC 20375, USA*

(Received 11 July 2005; published 8 November 2005)

A wedge or prism is a common geometry used in experiments involving left-handed media (LHM). It is shown that an exact analytical solution to the canonical problem of scattering by a LHM wedge or prism is feasible in the limit of no losses. The solution reproduces the ideal point image announced by Pendry which has not been observed experimentally. The analysis also results in the introduction of a new kind of resonator or photon localization device.

DOI: [10.1103/PhysRevE.72.056606](https://doi.org/10.1103/PhysRevE.72.056606)

PACS number(s): 42.70.Qs, 41.20.-q, 42.25.-p, 42.79.-e

Thirty-five years ago Veselago [1] proposed a hypothetical negative-index material also known as left-handed media (LHM), where the phase velocity and energy flow in opposite directions and where the vector trio  $\mathbf{E}$ ,  $\mathbf{H}$ , and  $\mathbf{E} \times \mathbf{H}$  form a left-handed orthogonal system. Pendry and Ramakrishna [2,3] argued that a LHM slab can amplify evanescent modes, allowing a complete reconstruction of a point source to a perfect point image, with none of the conventional optical limitations. The scarcity of materials available for experiments has contributed to considerable controversy over the expected optical properties for LHM. Although negative refraction is pretty much accepted in view of the recent experiments of Parazzoli *et al.* [4], and Houck *et al.* [5], one item that remains in controversy is superlensing: evanescent-wave considerations and simulations predict it [3,6,7]; however, measurements of LHM slabs show no evidence of it. It should be noted in this context that superlensing has recently been predicted analytically for some type of optically active media [8].

Experimental LHM materials have been composed of a periodic array of elements a fraction of a wavelength in size [9–12]. These materials are nonuniform and anisotropic; typically, a periodic array of split-ring resonators (SRR's) in combination with wires, of the type first proposed by Pendry *et al.* [13]. Such discreteness in the material, together with significant losses, has been blamed for the lack of confirmation of perfect focusing. Actually, even the ability to surpass the diffraction limit has also been questioned theoretically [14].

A shape that has been employed consistently in measurements of LHM optical properties is the wedge or angled prism [5,7,9]. Hence the problem of LHM wedge scattering under microwave horn illumination (or its equivalent, a line source) is of significant current interest. The LHM wedge is a scattering canonical shape which belongs to the class of penetrable objects for which it is assumed that an exact analytical solution is not possible [15,16] [only non penetrable wedges such as perfect electric conducting (PEC), perfect magnetic coupling (PMC), or characterized by an impedance boundary condition (in the manner of Maliuzhinets) do admit a solution].

It is shown in this paper that the ideal unit-index LHM wedge is an exception to the rule and admits an exact analytical solution to the scattering problem. In doing so, it is

proven that in the limit of negligible losses the solution does provide one with an ideal reconstruction of the image, just as envisioned by Pendry *et al.* as a side result, it is found that a metal-coated wedge, half filled with LHM and half empty, constitutes a new open resonator with photon localization characteristics. The analytical solution is validated against numerical experiments.

The geometry of the problem is shown in Fig. 1 for a wedge angle of  $2\alpha$ , and an electric line source is described by angle  $\theta_0$  and distance  $\rho_0$  from the vertex (the  $e^{-i\omega t}$  time convention is assumed and suppressed throughout). We are assuming  $\varepsilon = \mu = -1 + i\delta$  in the limit as  $\delta \rightarrow 0$ .

Edge illumination is critical and can be approximated by a local plane wave hitting the vertex. Here we find a paradox. This is illustrated in Fig. 2, which contemplates illumination of the top face of the wedge, by a bundle of rays coming from the source. Figure 2(a) depicts power flux arrows based on negative refraction (Snells' law) for matched LHM of index  $-1$ . As the angle  $\theta_0$  is decreased with respect to the scenario depicted by Fig. 2(a), the refracted bundle of rays will propagate in a direction that will approach the tangent vector of the wedge lower face. This is presented in Fig. 2(b), where the discontinuous nature of the power flow on the wedge lower face is deemed acceptable (this is consistent with polaritons, which can be used to mend a ray optics

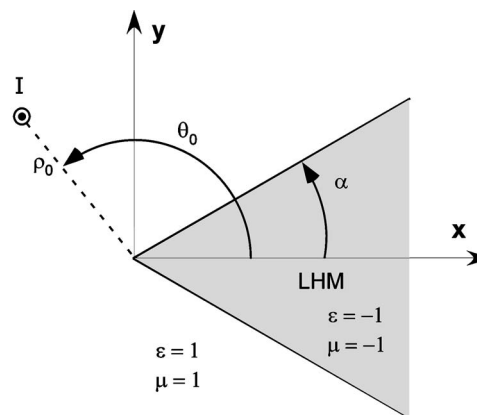


FIG. 1. Geometry of the problem. The wedge angle is  $2\alpha$ , and the line source is described by angle  $\theta_0$  and distance  $\rho_0$  from the vertex.

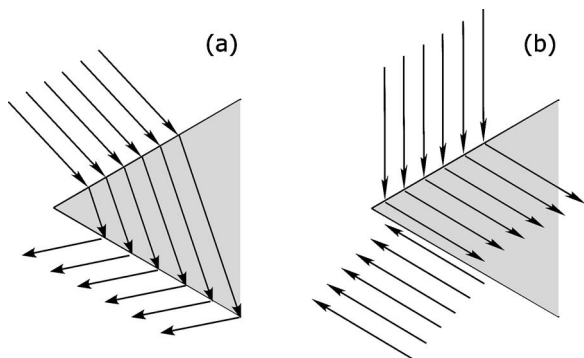


FIG. 2. Ray optical power flow picture applied to the wedge and used to restrict the incidence angle. (a) Acceptable scenario because double refraction is evident. (b) Double refraction occurs far away and emerging beam can be associated with an additional source, resulting in a paradoxical solution.

picture). As we approach such a critical angle of incidence, double refraction takes place farther and farther away from the vertex, and the absence of losses makes the full power come back, reminiscent of a source at infinity, as depicted by the lower arrows in Fig. 2(b), which make up the doubly refracted emerging beam.

It appears that a plane-wave solution of the scattering problem will be plagued by these paradoxical artificial sources. Since a line source can be seen as a bundle of plane waves, we expect the exact analytical solution for a line source to be constrained to incidence in such a way that the paradoxical situation is avoided. Making use of the ray picture presented above, it can be shown that incidence such that  $\theta_0 < 3\alpha$  leads to artificial sources. Accordingly and via use of symmetry, incidence is restricted here as follows:

$$3\alpha < \theta_0 < 2\pi - 3\alpha. \quad (1)$$

The problem is simplified by splitting it into two half-space even and odd parts. The field everywhere is built up of the superposition of the two solutions, which cancels the singularities that would have otherwise been present at the location of the mirror image of the original source. This is sketched in Fig. 3, where (a) illustrates the odd geometry with a PEC ground plane and (b) sketches the even geometry with a PMC ground plane.

First we analyze the odd case. As the electric field must be zero when the azimuth angle  $\theta=0$  and  $\theta=\pi$ , we expect solutions with angular dependence of the form  $\sin(\nu\theta)$  in the LHM wedge region and of the form  $\sin[\nu(\pi-\theta)]$  in the free-space region, for  $\nu$  is the parameter for the spectral or other-

wise general decomposition. Hence we propose

$$E_{\text{odd}} = \int_{\nu} d\nu \begin{cases} \frac{\sin(\nu\theta)}{\sin(\nu\alpha)} \Omega^{(1)}(\nu, k\rho), & \theta \in (0, \alpha), \\ \frac{\sin(\nu(\pi-\theta))}{\sin(\nu(\pi-\alpha))} \Omega^{(2)}(\nu, k_0\rho), & \theta \in (\alpha, \pi). \end{cases} \quad (2)$$

The radial functions  $\Omega^{(1)}(\nu, k\rho)$  and  $\Omega^{(2)}(\nu, k_0\rho)$ , solutions of the wave equation, need to be found so as to enforce continuity of the electric field across the material interface at  $\theta = \alpha$ . This is a problem with historical roots. The root of the problem is that phase continuity cannot be maintained with fully orthogonal radial eigenfunctions corresponding to dissimilar speed materials. For instance, for  $k_1 \neq k_2$  and assuming only ordinary materials, the function sets  $H_{\nu}^{(1)}(k_1\rho)$  and  $H_{\nu}^{(1)}(k_2\rho)$  are incompatible because a set of functions orthogonal to  $H_{\nu}^{(1)}(k_1\rho)$  will not be orthogonal to  $H_{\nu}^{(1)}(k_2\rho)$ , resulting in integral equations for the expansion coefficients, rather than closed-form expressions, as in the case of a PEC wedge [15].

The radiation condition in the free-space region dictates that for  $\rho > \rho_0$ ,  $\Omega^{(2)}(\nu, k_0\rho)$  must be of the form  $H_{\nu}^{(1)}(k_0\rho)$ . On the other hand, in the LHM wedge region, the radial solution for  $\rho > \rho_0$  must be a linear combination of  $H_{\nu}^{(1)}(k\rho)$  and  $H_{\nu}^{(2)}(k\rho)$ . In our case  $k = -k_0$ , and strictly speaking, using the fact that a causal solution requires  $\text{Im}(k) > 0$  and taking the limit of vanishing small losses indicates that, more precisely,  $k = k_0 e^{i\pi}$ . This is a critical detail in view of the branch cut  $(-\infty, 0)$  of the Hankel functions. The circuit relations for transitions to different functional branches across the branch cut can be shown to reduce to  $H_{\nu}^{(2)}(ze^{i\pi}) = e^{i\nu\pi} H_{\nu}^{(1)}(z) + 2 \cos(\nu\pi) H_{\nu}^{(2)}(z)$  and  $H_{\nu}^{(1)}(ze^{i\pi}) = -e^{-\nu\pi} H_{\nu}^{(2)}(z)$ . By using  $z = k_0\rho$ , the above leads to

$$H_{\nu}^{(1)}(k_0\rho) = e^{i\nu\pi} H_{\nu}^{(2)}(k\rho) + 2 \cos(\nu\pi) H_{\nu}^{(1)}(k\rho). \quad (3)$$

This equation is of critical importance because the right-hand side represents a valid solution in the LHM wedge region, whereas the left-hand side is a valid solution in the free-space region. This establishes a connection between the two solutions and enables us to enforce continuity across the interface. In view of Eq. (3), we can use  $H_{\nu}^{(1)}(k_0\rho)$  also as a radial solution in the LHM wedge region.

In the inner region where  $\rho < \rho_0$ , only Bessel functions are allowed because of energy integrability conditions. In a similar fashion, we can demonstrate that in the inner region, the eigenfunctions are related via  $J_{\nu}(k_0\rho) = e^{-i\nu\pi} J_{\nu}(k\rho)$ , indicat-

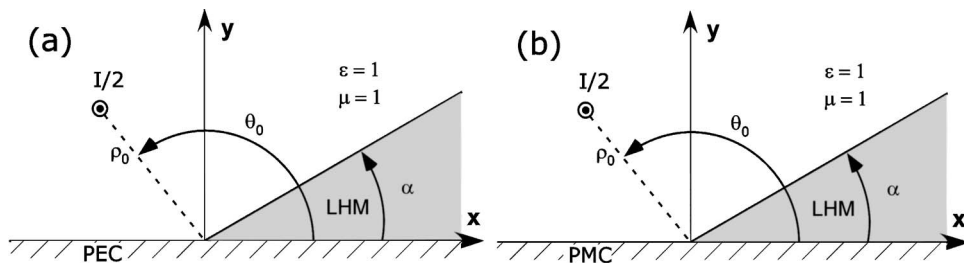


FIG. 3. Splitting of the problem into odd (a) and even (b) parts.

ing that we can use  $J_\nu(k_0\rho)$  in the inner region, both inside and outside the LHM wedge region. This simplifies matters greatly and enables us to obtain a closed-form solution to the problem at hand.

Hence we are left with

$$E_{\text{odd}} = \int_\nu d\nu \Psi(\nu) J_\nu(k_0\rho_{<}) H_\nu^{(1)}(k_0\rho_{>}) \times \begin{cases} \frac{\sin(\nu\theta)}{\sin(\nu\alpha)}, & \theta \in (0, \alpha), \\ \frac{\sin[\nu(\pi - \theta)]}{\sin[\nu(\pi - \alpha)]}, & \theta \in (\alpha, \pi), \end{cases} \quad (4)$$

where  $\rho_{<}$  and  $\rho_{>}$  denote the minimum and maximum of  $(\rho, \rho_0)$ . The equation maintains continuity of the electric field across the interface at  $\theta = \alpha$ , as well as across  $\rho = \rho_0$ , and satisfies the boundary conditions on the ground plane. The unknown spectral function  $\Psi(\nu)$  and range of integration will be obtained from satisfying the jump conditions in the magnetic field at the source location and the continuity of the radial magnetic field at  $\theta = \alpha$ .

From the identity  $H_\rho = (ik\eta\rho)^{-1} \partial E / \partial \theta$  we obtain via Eq. (4) that enforcement of the continuity of the radial magnetic field at  $\theta = \alpha$  results in

$$0 = \int_\nu d\nu \Psi(\nu) J_\nu(k_0\rho_{<}) H_\nu^{(1)}(k_0\rho_{>}) \{\cot(\nu\alpha) - \cot[\nu(\pi - \alpha)]\}. \quad (5)$$

On the other hand, using the identity  $H_\theta = -(ik\eta)^{-1} \partial E / \partial \rho$  and the fact that the jump in magnetic field is equal to the current according to  $I\delta(\theta - \theta_0) / 2\rho_0 = H_{\theta|\rho=\rho^+} - H_{\theta|\rho=\rho^-}$  leads to

$$\frac{I\pi k_0 \eta_0}{4} \delta(\theta - \theta_0) = \int_\nu d\nu \Psi(\nu) \times \begin{cases} \frac{\sin(\nu\theta)}{\sin(\nu\alpha)}, & \theta \in (0, \alpha), \\ -\frac{\sin[\nu(\pi - \theta)]}{\sin[\nu(\pi - \alpha)]}, & \theta \in (\alpha, \pi). \end{cases} \quad (6)$$

Note that we are using an extra factor of 1/2 because the odd current source has amplitude  $I/2$ . In deriving Eq. (6), use was made of the Wronskian function for cylinder functions [15].

To solve the system (5) and (6), we note that closure relations similar to Eq. (6) are exploited in the case of a PEC wedge, where the eigenvalues are discrete. Accordingly, we assume that the spectrum is discrete, from which Eq. (5) results in the eigenvalue equation  $\cot(\nu\alpha) = \cot[\nu(\pi - \alpha)]$ , which can be easily solved to yield

$$\nu = \frac{n\pi}{\pi - 2\alpha} \quad (7)$$

for  $n$  an arbitrary integer. Use of this in Eq. (6) results in

$$\begin{aligned} & \frac{I\pi k_0 \eta_0}{4} \delta(\theta - \theta_0) \\ &= \sum_n \frac{\Psi(\nu)}{\sin(\nu\alpha)} \begin{cases} \sin(\nu\theta), & \theta \in (0, \alpha), \\ -\sin[\nu(2\alpha - \theta)], & \theta \in (\alpha, \pi). \end{cases} \end{aligned} \quad (8)$$

By defining the functions  $S_\nu^{(\pm)}(\theta)$  as follows:

$$S_\nu^{(\pm)}(\theta) = A_\nu \begin{cases} \sin(\nu\theta), & \theta \in (0, \alpha), \\ \pm \sin[\nu(2\alpha - \theta)], & \theta \in (\alpha, \pi), \end{cases} \quad (9)$$

where  $A_\nu = \sqrt{\varepsilon_n / (\pi - 2\alpha)}$  and  $\varepsilon_n = 2$  for  $n = 1, 2, 3, \dots$ , except for  $\varepsilon_0 = 1$ . It can be shown that the following orthogonality identities are satisfied

$$\int_0^\pi d\theta S_\nu^{(\pm)}(\theta) S_\tau^{(\pm)}(\theta) \varpi(\theta) = \int_0^\pi d\theta S_\nu^{(+)}(\theta) S_\tau^{(-)}(\theta) = \delta_{n,m}. \quad (10)$$

Here  $\tau = m\pi / (\pi - 2\alpha)$  and  $\delta_{n,m}$  stands for the Kronecker delta, and the weighing function  $\varpi(\theta)$  is given by

$$\varpi(\theta) = \begin{cases} -1, & \theta \in (0, \alpha), \\ 1, & \theta \in (\alpha, \pi). \end{cases} \quad (11)$$

It appears that the discontinuous character of the weighing function is peculiar to LHM wedge regions.

Operating on Eq. (8) with  $\int_0^\pi d\theta S_\nu^{(+)}(\theta)$ , we obtain, upon using Eqs. (9) and (10),

$$\Psi(\nu) = \frac{I\pi k_0 \eta_0}{4} \sin(\nu\alpha) A_\nu S_\nu^{(+)}(\theta_0). \quad (12)$$

Use of this in Eq. (4) results in a compact expression for the odd-mode electric field:

$$E_{\text{odd}} = \frac{I\pi k_0 \eta_0}{4} \sum_n J_\nu(k_0\rho_{<}) H_\nu^{(1)}(k_0\rho_{>}) S_\nu^{(+)}(\theta_0) S_\nu^{(+)}(\theta). \quad (13)$$

Here the sum is extended over all positive integers  $n$  (there is no contribution from the  $n=0$  term).

The even solution can be obtained by similar means; here, we just quote the final result

$$E_{\text{even}} = \frac{I\pi k_0 \eta_0}{4} \sum_n J_\nu(k_0\rho_{<}) H_\nu^{(1)}(k_0\rho_{>}) C_\nu^{(+)}(\theta_0) C_\nu^{(+)}(\theta), \quad (14)$$

where now there is contribution from the  $n=0$  term; furthermore,

$$C_\nu^{(\pm)}(\theta) = A_\nu \begin{cases} \cos(\nu\theta), & \theta \in (0, \alpha), \\ \pm \cos[\nu(2\alpha - \theta)], & \theta \in (\alpha, \pi), \end{cases} \quad (15)$$

and the coefficient  $A_\nu$  is the same one introduced in the odd case.

The final solution is obtained by simply adding the even and odd contributions from Eqs. (13) and (14), respectively; we obtain



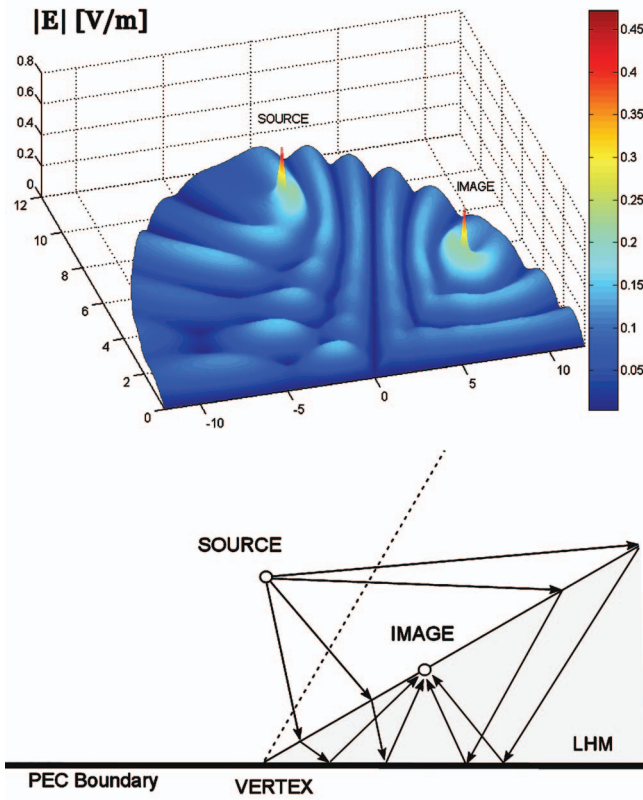


FIG. 4. (Color) **E**-polarized line source excitation on wedge of angle  $\alpha$  on top of a ground plane) with  $\alpha=30^\circ$ ,  $\theta_0=90^\circ$ ,  $f=10$  GHz ( $\lambda=3$  cm), and  $\rho_0=9$  cm. (a) Series solution showing **E** field amplitude (rms) and (b) ray optics description of image formation showing nodal plane (dotted line).

$$E = -\frac{I\pi k_0 \eta_0}{4} \sum_{n=0}^{\infty} J_\nu(k_0 \rho_{<}) H_\nu^{(1)}(k_0 \rho_{>}) \times A_v^2 \begin{cases} \cos\{\nu[2\alpha - (\theta + \theta_0)]\}, & \theta \in (-\alpha, \alpha), \\ \cos\{\nu(\theta - \theta_0)\}, & \theta \in (\alpha, 2\pi - \alpha). \end{cases} \quad (16)$$

This is the exact solution for the total electric field, for

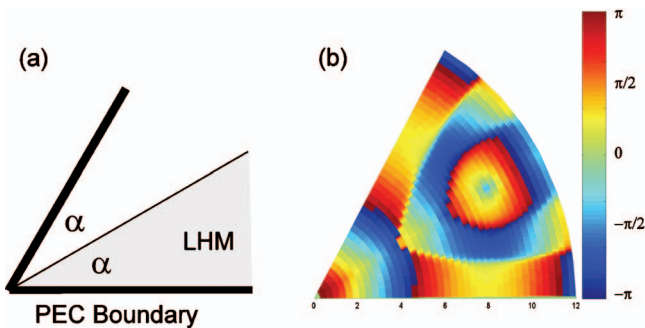


FIG. 5. (Color) Photon localization by means of a PEC internal wedge of angle  $2\alpha$  containing a LHM wedge of angle  $\alpha$ . (a) Geometry (b) Phase series solution corresponding to  $\alpha=30^\circ$ ,  $f=10$  GHz ( $\lambda=3$  cm), and  $\rho_0=9$  cm. Ray tracing can also be used to show localization in the wedge region.

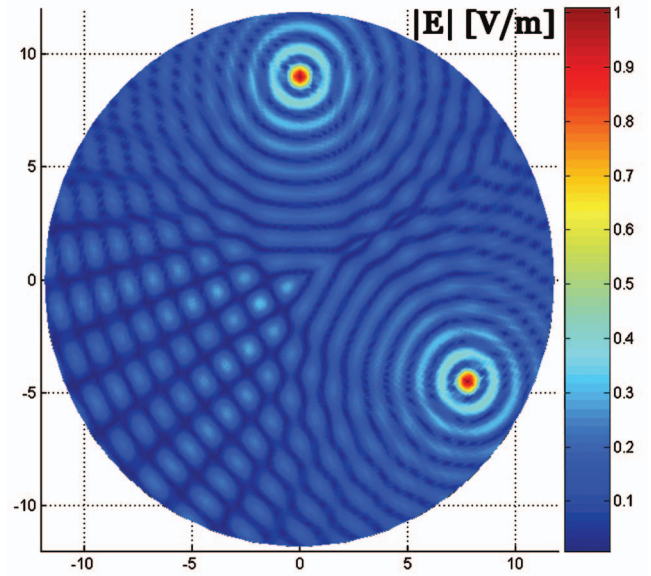


FIG. 6. (Color) Magnitude of the time-harmonic field  $|E(t)|$  for  $\alpha=30^\circ$ ,  $\theta_0=90^\circ$ ,  $\rho_0=9$  cm, and  $f=15$  GHz. Series solution (normalized). The vertex is at the center of the polar graph.

**E**-polarized line source excitation, and is valid everywhere; in free space and in the LHM wedge.

Since exact solutions for penetrable materials are virtually nonexistent, the above solution is a significant addition to the theory of diffraction by material wedges. The solution is also applicable to **H**-polarized (magnetic) line source excitation, in which case Eq. (16) represents the total axial **H** field. This extension comes from recognizing that the LHM wedge is self-dual and that under duality  $\mathbf{E} \rightarrow \mathbf{H}$ ,  $\mathbf{H} \rightarrow -\mathbf{E}$ , and  $\mu \leftrightarrow \epsilon$ . Hence, application of duality to the present configuration translates directly into the **H**-polarization problem.

The above solution has been implemented numerically, and a few representative calculations follow together with a discussion of the physics behind the solution. In the series

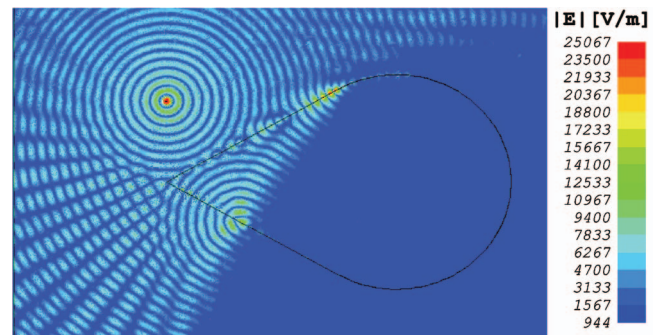


FIG. 7. (Color) HFSS solution for a slightly lossy LHM wedge cylinder. Magnitude of the time-harmonic field  $|E(t)|$  for  $\alpha=30^\circ$ ,  $\theta_0=90^\circ$ ,  $\rho_0=9$  cm,  $f=15$  GHz,  $\epsilon=\mu=-1+i0.001$ , distance from vertex to circle center of 24 cm, and circle radius 12 cm (flat wedge side  $\sim 20.78$  cm). The smooth finite structure reduces the disturbance of the required polaritons (a disruption is present at the point of discontinuity in curvature). In spite of the finiteness of the model, the image appears at the interface just as predicted by the series solution.

calculations we are setting  $-ik_0\eta_0/4=1$  for convenience.

Our first example is given by an odd geometry (wedge of angle  $\alpha$  on top of a ground plane) with  $\alpha=30^\circ$ ,  $\theta_0=90^\circ$ ,  $f=10$  GHz ( $\lambda=3$  cm), and  $\rho_0=9$  cm. The electric field amplitude (rms) was calculated via the series solution for  $\rho \leq 12$  cm (convergence was reached), and the solution is presented in Fig. 4(a). The geometry was chosen because, since  $\theta_0=3\alpha$ , the image, as dictated by ray optics, occurs at the LHM interface at the distance  $\rho_0$  from the vertex [see Fig. 4(b) for ray tracing]. However, reflection on the conducting boundary adds a  $180^\circ$  phase shift on the image, and since source and image behave as equal-amplitude sources on the interspace between them, the oddness of the electric field results in a nodal line being formed at  $\theta=60^\circ$ . The nodal line is evident in the simulations.

The above example illustrates the existence of a nodal plane. Since for **E** polarization a nodal plane can be replaced by a conductor, we have that the reduced geometry within the metal walls is characterized by a sourceless (nonforced) solution of the field equations and hence constitutes an open resonant cavity or photon localization device. This is illustrated in Fig. 5(a) which shows the resulting PEC internal wedge of angle  $2\alpha$  containing the LHM wedge of angle  $\alpha$ . For completeness, the series solution for the phase is presented in Fig. 5(b) corresponding to  $\alpha=30^\circ$ ,  $f=10$  GHz ( $\lambda=3$  cm), and  $\rho_0=9$  cm. The phase surface shows a smooth valley at the location of the image, which indicates that the phase velocity (aligned with the phase gradient) points towards the source in all directions. This is correct because the image is at the air-LHM interface and power is opposite to phase on the LHM side, indicating that power flows by the

location of the image (which is not a source). Localization in the wedge region can also be shown via ray optics (not shown), as any ray emitted from a point on the interface region travels back in phase to the place of origin after a trip consisting of a single refraction (air-LHM interface) and double reflection at the PEC walls ( $2\pi$  phase shift).

Our final example is afforded by a line source **E** polarization with the same previous parameters ( $\alpha=30^\circ$ ,  $\theta_0=90^\circ$ ,  $\rho_0=9$  cm), but  $f=15$  GHz, and for a wedge in free space (full solution). The ray optics picture calls for an image at the location of the lower air-LHM interface at a distance  $\rho_0$  from the vertex, and this is precisely what is observed by the series solution shown in Fig. 6, which shows the magnitude of the time-harmonic field  $|E(t)|$ , which has been obtained by simply taking the magnitude of the real part of Eq. (16). This solution has been validated against an HFSS (Ansoft) model on a smooth wedge cylinder as representative of the local wedge geometry. HFSS can only model a finite wedge, and without the smooth rounding provided by the cylindrical portion, reflections off the ends would disturb the proper excitation of polaritons (some disruption is still present at the place of a higher-order discontinuity, the discontinuity in curvature). In addition, since HFSS employs real lossy parameters  $\epsilon=\mu=-1+i0.001$ , the calculation serves to validate our analytical solution as the correct limiting solution in absence of losses. The agreement is very good (see Fig. 7).

To summarize, an exact analytical solution to the canonical problem of scattering by a left-handed wedge or prism has been found in the limit of no losses. The solution reproduces the ideal point image announced by Pendry *et al.* The analysis also resulted in the introduction of a new kind of resonator or photon localization device.

- 
- [1] V. G. Veselago, *Sov. Phys. Usp.* **10**, 509 (1968).  
 [2] J. B. Pendry and S. A. Ramakrishna, *J. Phys.: Condens. Matter* **14**, 8463 (2002).  
 [3] J. B. Pendry, *Phys. Rev. Lett.* **85**, 3966 (2000).  
 [4] C. G. Parazzoli, R. B. Gregor, K. Li, B. E. C. Koltenbah, and M. Tanielian, *Phys. Rev. Lett.* **90**, 107401 (2003).  
 [5] A. A. Houck, J. B. Brock, and I. L. Chuang, *Phys. Rev. Lett.* **90**, 137401 (2003).  
 [6] D. R. Smith, D. Schurig, M. Rosenbluth, S. Schultz, S. A. Ramakrishna, and J. B. Pendry, *Appl. Phys. Lett.* **82**, 1506 (2003).  
 [7] X. S. Rao and C. K. Ong., *Phys. Rev. E* **68**, 067601 (2003).  
 [8] Cesar Monzon and D. W. Forester, *Phys. Rev. Lett.* **95**, 123904 (2005).  
 [9] R. A. Shelby, D. R. Smith, and S. Schultz, *Science* **292**, 77 (2001).  
 [10] D. R. Smith, W. J. Padilla, D. C. Vier, S. C. Nemat-Nasser, and S. Schultz, *Phys. Rev. Lett.* **84**, 4184-41877 (2000).  
 [11] R. A. Shelby, D. R. Smith, S. C. Nemat-Nasser, and S. Schultz, *Appl. Phys. Lett.* **78**, 489-491 (2001).  
 [12] F. J. Rachford, D. L. Smith, P. F. Loschialpo, and D. W. Forester, *Phys. Rev. E* **66**, 036613 (2002).  
 [13] J. B. Pendry, A. J. Holden, D. J. Robbins, and W. J. Stewart, *IEEE Trans. Microwave Theory Tech.* **47**, 2075 (1999).  
 [14] N. Garcia and M. Nieto-Vesperinas, *Phys. Rev. Lett.* **88**, 207403 (2002).  
 [15] D. S. Jones, *The Theory of Electromagnetism* (MacMillan, New York, 1964).  
 [16] *Radar Cross Section Handbook*, edited by G. T. Ruck (Plenum Press, New York, 1970).